

INJECTION AND EXTRACTION FOR THE EMMA NS-FFAG

K. Marinov, S. I. Tzenov and B. D. Muratori,
STFC Daresbury Laboratory and Cockcroft Institute, UK

Abstract

EMMA (Electron Machine with Many Applications) is a prototype non-scaling electron FFAG being commissioned at Daresbury Laboratory. Ns-FFAGs have great potential for a range of new applications in many areas of science, technology, manufacturing and medical applications including the next generation high energy proton and heavy ion accelerators for accurate and effective particle beams cancer therapy, muon accelerators for the study of the physics and chemistry of advanced materials and accelerator driven subcritical reactors (ADSRs). This paper summarizes the design of the extraction and injection transfer lines of EMMA as well as the associated septa and kickers. The ALICE energy recovery linac prototype is used as the injector to EMMA, with energy range from 10 to 20 MeV. Because this is the first non-scaling FFAG constructed, it is crucial to study as many of the electron beam properties as feasible, both at injection and after acceleration in an extraction line. To do this, a complex injection line was designed consisting of a dogleg to extract the beam from ALICE, a matching section, a tomography section and some additional dipoles and quadrupoles to transport the beam to the entrance of EMMA. Similarly the design of the extraction line and its diagnostics are described.

INTRODUCTION

EMMA is currently being commissioned at Daresbury Laboratory, UK, to demonstrate the world's first operation of a new concept in accelerator design called non-scaling FFAG, (ns-FFAG) [1,2]. Ns-FFAGs were first designed to provide very rapid acceleration for muon beams and have since been further developed for a wide range of potential applications. These range from the next generation high energy proton and heavy ion accelerators for accurate and effective particle beam cancer therapy (PAMELA [3]), an accelerator for a muon facility for the study of the physics and chemistry of advanced materials, to accelerator driven subcritical reactors (ADSRs). In ADSRs, fission is enabled by high energy proton beams spallating neutrons from a target embedded in a thorium fuelled reactor [4]. Ns-FFAGs have also been adopted as the baseline design for an international neutrino factory [5]. First, the "proof of principle" accelerator EMMA must be demonstrated, this is summarised in [6].

INJECTION LINE

The ALICE to EMMA injection line, shown in Figure 1, consists of a dogleg to extract the beam from the ALICE accelerator, a tomography section and finally a short dispersive section consisting of two dipoles, prior to

the injection septum [7]. After the dogleg, the beam is matched into a tomography diagnostic via four quadrupoles. The purpose of this section is twofold: Firstly, to provide a quick and precise measurement of the Twiss parameters, and secondly to make emittance and transverse profile measurements. This creates a 'fixed point' in the line after which, if the tomography section is matched correctly, the Twiss parameters at all energies should be the same. This is useful because of the requirement to inject at a range of energies, which gives different Twiss parameters depending on the amount of RF focusing from the ALICE linac cavities and how far off-crest they are. The rest of the line after the tomography section can then be used to optimise the slightly different, energy dependent, injection parameters.

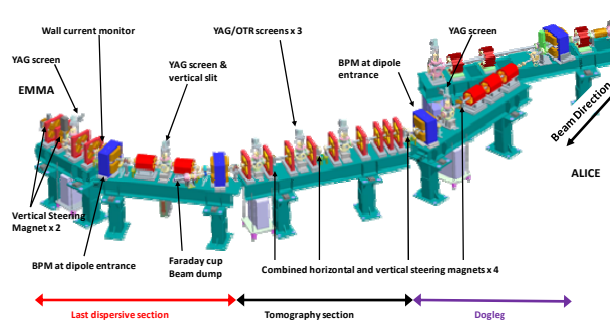


Figure 1: ALICE to EMMA injection line.

In order to improve the study of the physics of ns-FFAGs, it is important to minimise the energy spread of the beam at the start of the injection line. By carefully choosing the phases of the two ALICE linac cavities, it was possible to achieve an energy spread less than 0.05 % (5 keV at 15 MeV). This has not yet been repeated at all other energies but there is no reason to think it will not be possible to achieve the same as all that is done is a simple elimination of the correlated energy spread and the uncorrelated one remains constant.

MODELLING

The results reported in this section are from the tracking code FFEMMAG developed S. Tzenov at Daresbury Laboratory and described in [8]. Other studies of injection and extraction into the EMMA ring [9,10] using different codes give broadly similar results.

Single Turn Injection

The basic elements of the injection system are a septum magnet and two kicker magnets, located in two successive long straight sections immediately after the long straight section where the septum is inserted. The extraction system is simply a mirror image of the injection one.

Since after injection the beam passes through the kicker many times, it is desirable that there is no residual kicker field acting on the beam during the successive passes. The initial kicker design assumed such a perfect scheme, where the magnetic field vanishes after one turn, which is approximately within 55 nanoseconds.

In the ideal case of one-turn injection, the magnetic field of the two kickers drops to zero within 55 nanoseconds. The injection simulation is performed by tracking the injection orbit of a reference particle backwards from a point on the reference trajectory after the second kicker to the septum magnet. An example of one-turn injection at 10 MeV is shown on Figure 2 below.

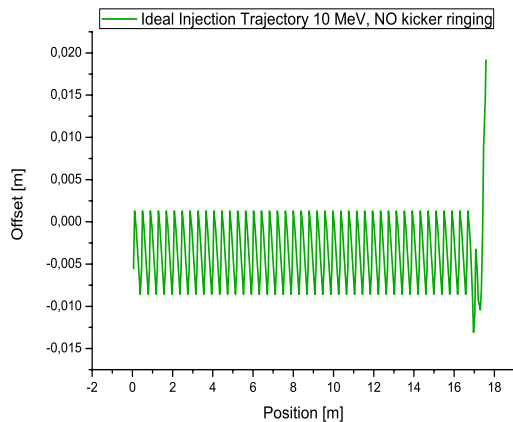


Figure 2: Ideal injection trajectory at 10 MeV. Kicker field acts only during the first turn.

If the kicker field during the second turn drops to less than one percent of the peak field, then there is practically no difference between the corresponding injection trajectory and the ideal one. This is shown in Figure 3.

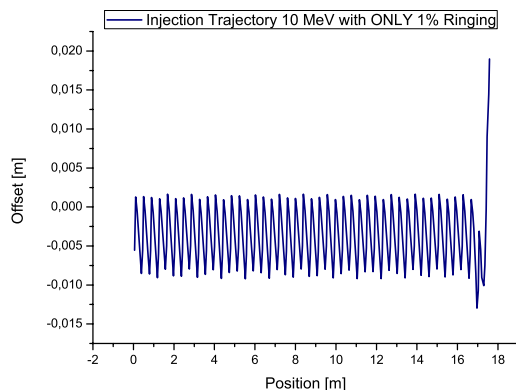


Figure 3: Trajectory at 10 MeV with a kicker field of one percent of the peak field during the second turn.

Multi-turn Injection

The technical challenge of building a kicker and power supply that give a maximum field of less than one percent of the peak magnetic field for subsequent turns (that is after 55 nanoseconds) has so far not been achieved. The field falls exponentially in time after the peak, but is still

about 10% of the peak value during the second pass of the beam through the kicker, an order of magnitude greater than the tolerance required for single turn injection. The measured kicker field as a function of time is shown in Figure 4.

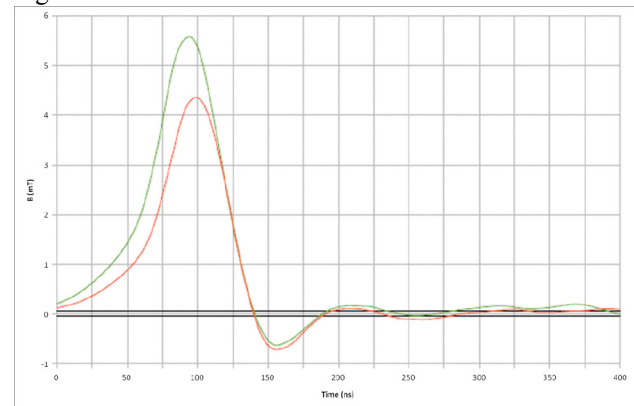


Figure 4: Magnetic field vs. time for two different excitation voltages (20 KV and 26 KV). Closed orbit of first turn with ringing $\pm 1\%$ limits shown in black.

Thus it is now necessary to adopt a multi-turn injection in a ns-FFAG. A clear way to realize such a scheme is to abandon the principle that the beam should be placed on the reference trajectory after the first pass through both kickers. It turns out that after the first pass particles could be injected on an orbit sufficiently close to the reference trajectory that the residual kicker magnetic field places the particles on the true equilibrium orbit during the second turn. The primary restriction on this scheme is the requirement that any trajectory excursion should remain well within the physical aperture of the machine.

Modelling of multi-turn injection involves two passes of the beam through the kicker fields. During the first pass they are set to their nominal value and are fired at the right time, while during the second pass their amplitude and polarity is determined by the characteristics of the kicker and power supply. For modelling purposes, the field is assumed to have reduced to 10% of peak with reversed polarity for the second turn. Figure 5 shows the results of the simulation for 10 MeV with 10% ringing.

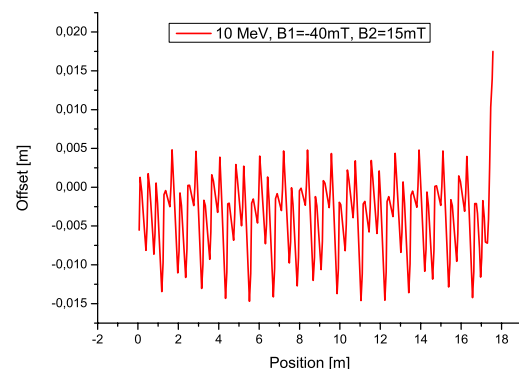


Figure 5: Two turn injection trajectory at 10 MeV with 10% kicker ringing.

During the first turn the beam moves along a trajectory that is not the correct periodic reference orbit corresponding to its energy. Therefore, as one should expect, the amplitude of the beam oscillations are larger than the ones associated with the equilibrium orbit. Figures 6 and 7 show the minimum and the maximum deviations of the trajectory with respect to the polygon centre line (approximately equivalent to the 15 MeV orbit) as a function of energy.

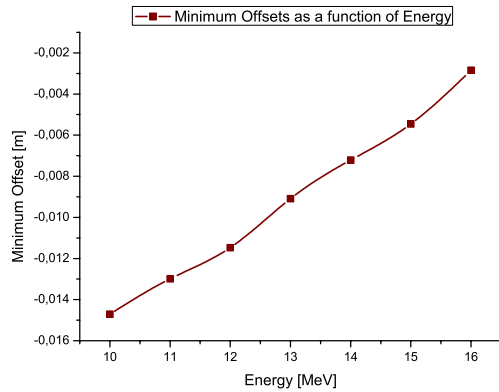


Figure 6: Minimum deviation of the trajectory versus energy due to kicker field ringing of 10%.

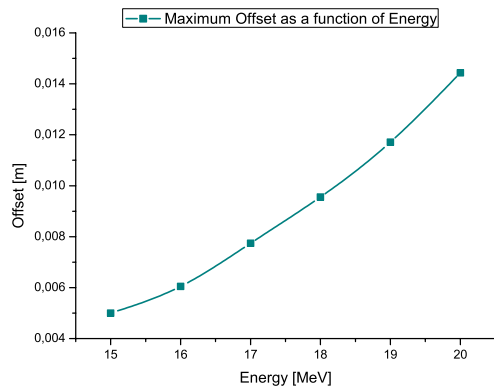


Figure 7: Maximum deviation of the trajectory versus energy due to kicker field ringing of 10%.

EMMA PULSED MAGNETS

Both the EMMA injection and the extraction systems consist of a septum and two kickers. Apart from the kicker's power supply units (PSUs), these devices are designed, manufactured and tested at Daresbury Laboratory.

Septa

The EMMA septa are eddy-current type, in-vacuum magnets that provide the necessarily large bending angles (65° for injection and 70° for extraction) within less than 10 cm of physical magnet length. These are two identical, movable magnets, capable of radial translation and rotation around their centre in order to enable injection and extraction over the entire energy range of interest (10

to 20 MeV) as shown in Figure 8.

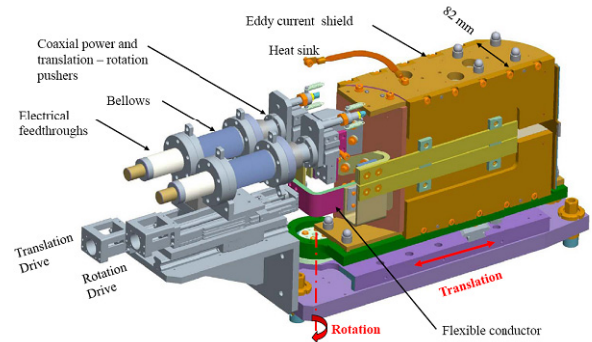


Figure 8: Septum design with actuators for translation and rotation.

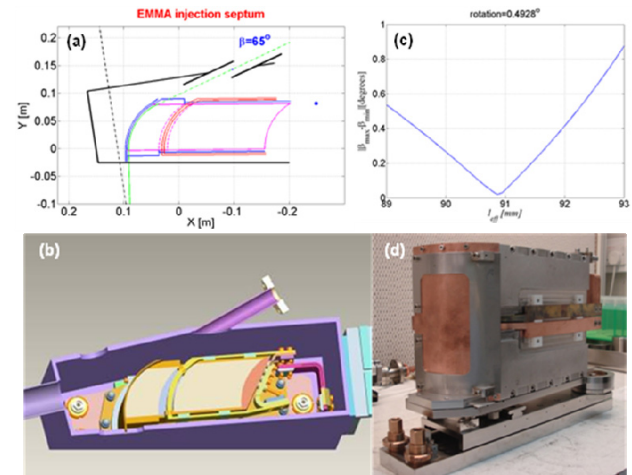


Figure 9: EMMA injection septum. (a) Concept. The vacuum vessel is shown in black, eddy-current screen – blue, magnetic steel – purple, magnetizing coil – red. The blue dot is the pivot point. (b) CAD model (c) Determining the effective length of the magnet (d) The assembled magnet before installation.

In order to ensure that the available space is used efficiently the geometry of the problem was studied in detail by creating a MATLAB model of the magnet and its vacuum vessel, Figure 9 (a). This allowed the optimum pole area, radius of curvature and magnet position to be determined to ensure the necessary clearance between the magnet, the beam and the vacuum vessel. In addition the location of the rotation centre and the necessary ranges of rotation and translation were also assessed, based on a large number of injection and extraction scenarios. This was followed by an extensive three-dimensional (3D) ELEKTRA modelling, with the purpose of determining the field quality and particularly in decreasing the stray field strength. Various configurations were considered and their performance was judged against the feasibility of the design.

The magnets have been assembled from a stack of wire-eroded, 0.1 mm thick laminations constructed of Cogent Surahammars Bruks No. 10 grade electrical steel (<http://www.sura.se>) A filling factor of the order of 96% to 97% has been achieved and a two-turn magnetizing

coil has been implemented in order to reduce the required current. A number of tests were performed on the assembled septa before installation. A detailed 3D map of the magnetic field was measured. Stray field strength has been reduced as much as possible by improving the electrical contact between the various components of the eddy-current screen. This has been achieved by both using the (experimentally determined) optimum amount of torque on the screws that hold the eddy-current screen in place and by adding additional copper plates at appropriate positions. Overall, this procedure resulted in a three-fold reduction of the integrated stray field strength, compared to the value that was measured immediately after the unit was assembled for the first time.

In the very early stages of the EMMA commissioning work the performance of the installed injection septum magnet was tested by measuring the dependence of the beam angle immediately after the septum $\alpha(B_N)$ on the nominal septum field strength B_N .

Indeed, it can be shown that the angle of incidence β is given as:

$$\beta = \sin^{-1} \left[B_N e l_{\text{eff}} c \left(E \sqrt{1 - \left(\frac{E_0}{E} \right)^2} \right)^{-1} - \sin(\alpha(B_N) + \varphi) \right] + \varphi \quad (1)$$

Where $l_{\text{eff}} = \int_{-\infty}^{\infty} B(y) dy / B_N$ is the effective length of the magnet, φ is the angle of magnet rotation, E is electron beam energy, E_0 is the rest energy of the electron and e and c are the electron charge and the speed of light respectively. Clearly, since β is fixed, substitution of the experimentally determined function $\alpha(B_N)$ (and the correct value of l_{eff}) in (1) should result in the same value of β for every value of B_N in the entire range of magnetic field strength values covered experimentally. Therefore by treating l_{eff} in (1) as a parameter a simple fitting procedure can be implemented to determine the value of the effective magnetic length. Indeed, the variation $\Delta\beta(l_{\text{eff}}) = \beta_{\text{max}} - \beta_{\text{min}}$ resulting from (1) versus the corresponding value of the parameter l_{eff} can be easily obtained. Then the value of l_{eff} at which $\Delta\beta$ reaches a minimum is the effective length of the magnet. As Fig. 1(c) shows the resulting value is $l_{\text{eff}} = 90.9$ mm. On the other hand using the definition l_{eff} and the measured field distribution $B(y)$ results in $l_{\text{eff}} = 91.4$ mm. The good agreement between the two procedures shows that the septum performs as designed.

Kickers

The EMMA kickers are inductive, in-vacuum devices required to reach peak integrated field strength of 0.007 Tm with field rise/fall time less than the EMMA revolution time of ~ 55 ns for extraction/injection. The magnet consists of a C-shaped, CMD5005-type ferrite core held in place by a system of springs and magnetized by a single-turn conductor, Figure 10. The ability to conduct magnetic tests in air prior to installation was a design requirement and in order to achieve this a minimum distance of 15 mm between any two metal parts

not in direct electric contact with each other was implemented. A detailed 3D ELEKTRA model was created to determine the field quality and the effective magnetic length. Particular attention has been paid to minimizing the ratio between stray and magnet inductance. The magnets are fitted with in-situ field probes (single-turn wire loops) in order to monitor and adjust the temporal field profile during operation. The magnets were subjected to extensive testing and measurement process before installation.

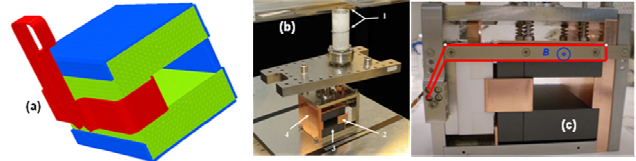


Figure 10: EMMA kicker (a) ELEKTRA model. Green – CMD5005-type ferrite, blue – copper screen, red – magnetizing coil. The gap height is 25 mm and the magnet length is 100 mm. (b) The assembled magnet. 1 – co-axial vacuum feed-through, 2 – magnetizing coil, 3 – ferrite core, 4 – copper screen. (c) The in-situ field probe.

PULSED MAGNETS COMMISSIONING

The operation of the pulsed magnets has gone quite well so far. The position and angle of the injected bunch were measured after the exit of the septum and hence the orbit was reconstructed. The required strength of two kickers to take the beam on to the design orbit was then calculated and is shown in Figure 11. The calculated kicker strength is not exactly the same as the measured values but is similar.

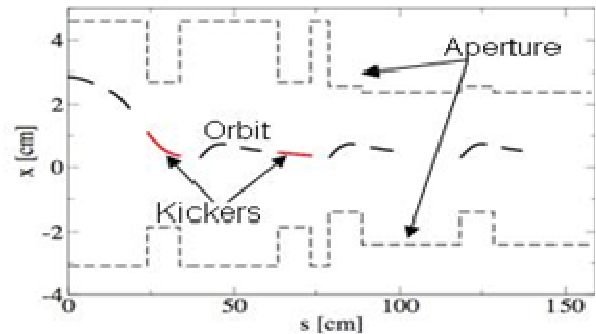


Figure 11: Injection region orbit, two normal cells (courtesy D. Kelliher).

EXTRACTION LINE

The primary purpose of the EMMA extraction line is to make diagnostic measurements that cannot be made within the ring. It is therefore, necessary for this line to be able to transport any energy from 10 to 20 MeV, with the beam coming from the full acceptance of the ring. It consists of an extraction septum with the dispersion closed by quadrupole magnets and an additional dipole forming an irregular dogleg arrangement, as shown in Figure 12.

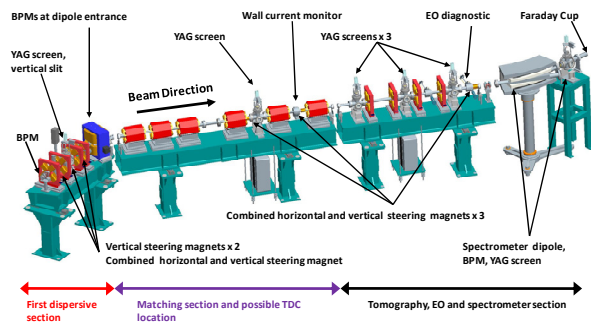


Figure 12: EMMA extraction line.

As part of this irregular dogleg, there is an YAG screen whose function it is to measure the energy, together with an additional screen in the following dispersion-free straight. In the straight following the dogleg are quadrupole magnets to match the beam either directly into a tomography section or into a proposed transverse deflecting cavity. The tomography section is identical to that in the injection line, thus allowing the effect EMMA has on the projected transverse emittance and the transverse profiles to be determined. The transverse deflecting cavity can be used to measure bunch length and projected transverse slice emittance to determine the longitudinal profile of the bunch. After the tomography section there is a spectrometer dipole to measure the energy of the beam. If the bunch is “streaked” using the deflecting cavity, then it will also be possible to measure the longitudinal energy spread of the beam. Between the tomography section and the spectrometer dipole, there will be an Electro Optic (EO) diagnostic to measure the bunch length and longitudinal profile [11].

FUTURE COMMISSIONING PLANS

The current commissioning shifts are dedicated to accelerator physics and RF studies; a recent detailed summary may be found in [12].

The beam from ALICE is kept at a fixed energy and an equivalent lattice is created in the EMMA ring by scaling the magnet fields. This means, strictly equivalent settings can be used in the injection line set-up and this need only be done once at a specific energy between 10 and 20 MeV. Eventually, of course, the complete set-up needs to be done, at 1 or 0.5 MeV steps. We intend to measure the time of flight (ToF) for each equivalent lattice in order to map out the predicted parabolic behaviour of this with energy. The LLRF system for EMMA also needs to be commissioned with specific care given to the cavity tuning to ensure phase and amplitude stability over the required range of frequencies (1.3 GHz + 1.5 /- 4.0 MHz). Having achieved this, we hope to have a verification of successful acceleration, evidence of energy gain from acceleration inside and then outside of the bucket, soon after.

Finally, everything described above shall be repeated at the real (as opposed to equivalent) energies from 10 to 20 MeV and the bunch will be extracted down the extraction line, in order to be able to diagnose in detail the effects

EMMA has had on the beam.

SUMMARY

EMMA is the world’s first ns-FFAG and injection and extraction are two of the most challenging aspects. The most challenging of all is the construction and operation of the pulsed magnets, all of which were designed and constructed locally at Daresbury Laboratory. A brief overview of the approach to both injection and extraction was given and the major problems encountered highlighted.

After a brief description of the prerequisites and basic reasons to adopt a multi-turn injection scheme, some tracking results concerning the beam dynamics for injection matching have been shown. These results indicate that the latter is feasible within reasonable aperture and strength specifications of the septum and kicker magnets.

ACKNOWLEDGEMENTS

We would like to acknowledge the entire EMMA team for their help and useful discussions.

REFERENCES

- [1] S. L. Smith, “EMMA, the World’s First Non-Scaling FFAG Accelerator”, Proc. PAC09, Vancouver, BC, Canada (2009).
- [2] R. Edgecock, Proc. IPAC10, Kyoto, Japan, (2010).
- [3] K. Peach et al, “PAMELA Overview: Design Goals and Principles”, Proc. of PAC09, Vancouver, BC, Canada (2009).
- [4] C. Bungau, R. J. Barlow, R. Cywinski, “Reactor Design Studies for an Accelerator Driven System”, Proc. of PAC09, Vancouver, BC, Canada (2009).
- [5] K. Long (Ed), “An International Scoping Study of a Neutrino Factory and Super-beam Facility”, CARE-Report-2005-024-BENE, (2005).
- [6] J. S. Berg, “The EMMA Main Ring Lattice”. CONFORM report conform-emma-acc-rpt-0001-v1.2-jsberg-lattice (2008).
- [7] B.D. Muratori et al., ‘Injection and Extraction for the EMMA NS-FFAG’, Proc. EPAC08, Genoa (2008).
- [8] J. K. Jones, B. D. Muratori, S. L. Smith and S. I. Tzenov, “Dynamics of Particles in Non-Scaling FFAG Accelerators”. Progress in Physics, Vol. 1 72-82 (2010).
- [9] J. S. Berg, “An Injection/Extraction Scenario for EMMA”, Proc. PAC09, Vancouver, Canada (2009).
- [10] Y. Giboudot, D. Kelliher, F. Méot and T. Yokoi, “Beam Dynamics Simulations Regarding the Experimental FFAG EMMA, Using the On-line Code”. Proc. IPAC2010, Kyoto, Japan (2010).
- [11] G. Berden et al, Proc. EPAC04, Lucerne, Switzerland (2004).
- [12] S. Smith, “First Commissioning Results from the Non-Scaling FFAG accelerator, EMMA”. Proc. Cyclotrons2010, Lanzhou, China (2010).